RESEARCH

Vol. 16, 2019

ISSN 2319–7757 EISSN 2319–7765

Indian Journal of Engineering

Design and fabrication of insulation testing rig

Nnamchi SN[1]✉, Nnamchi OA[2], Sangotayo EO[3], Mundu MM[4], Edosa OO[5]

1. Department of Mechanical Engineering, SEAS, Kampala International University, Ggaba Road, Kansanga, P.O.B 20000 Kampala, Uganda, Email: stephen.nnamchi@kiu.ac.ug: https://orcid.org/0000-0002-6368-2913
2. Department of Agricultural Engineering, Michael Okpara University of Agriculture, Umudike, Umuahia, Nigeria, Email: onyxhoni@yahoo.com
3. Department of Mechanical Engineering, SEAS, Kampala International University, Ggaba Road, Kansanga, P.O.B 20000 Kampala, Uganda, Email: sangotayo.emmanuel@kiu.ac.ug.
4. Department of Physical Sciences, SEAS, Kampala International University, Ggaba Road, Kansanga, P.O.B 20000 Kampala, Uganda, Email: mundumustafa@yahoo.com
5. Department of Mechanical Engineering, SEAS, Kampala International University, Ggaba Road, Kansanga, P.O.B 20000 Kampala, Uganda, Email: osaruene@kiu.ac.ug

✉**Corresponding author:**
S.N. Nnamchi
Department of Mechanical Engineering, KIU,
Kampala, Uganda
E-mail: stephen.nnamchi@kiu.ac.ug; nnasteve@yahoo.com

Biographies:

Stephen Ndubuisi Nnamchi is currently a Senior Lecturer in Mechanical Engineering Department with specialty in Thermofluid Engineering and Renewable Energy System at Kampala International University, Kampala Uganda. He holds dual M.Eng in Mechanical and Chemical Engineering, and PhD in Mechanical Engineering (Thermofluids) at University of Port Harcourt, Port Harcourt, Nigeria in 2001, 2005 and 2014, respectively. He has over 12 years of post-qualification experience in teaching, learning and research in applied thermofluid, research methods, thermodynamics, momentum/heat/mass transfer and alternative energy systems. He holds IWCF supervisory certificate in rotary well drilling, 2013; and practical experience in oil and gas industry, which blends with his academic experience.

Onyinyechi Adanma Nnamchi is currently a postgraduate student of Food Engineering and Bio Process in Department of Agricultural Engineering, Michael Okpara University of Agriculture, Umudike, Nigeria. She holds B.Eng in Chemical Engineering from Federal University of Technology, Owerri in 2011. She is currently carrying out her thesis under the co-supervision of *Stephen Ndubuisi Nnamchi* on solar thermal system. She has carried out project on characterisation of clays for thermal treatment of vegetable oil and has shown keen interest in design and performance analysis of thermal systems.

*Emmanuel O. Sangotayo,*is a Lecturer at the Department of Mechanical Engineering, Ladoke Akintola University of Technology, Ogbomoso. He holds a Bachelor of Technology (B.Tech. 2003) and Master of Technology (M.Tech., 2008) in Mechanical Engineering from the Ladoke Akintola University of Technology, Ogbomoso, Nigeria. He had a Ph.D. degree, in Mechanical Engineering (PhD, 2017) at Federal University of Agriculture, Abeokuta, Nigeria. His research interests are in thermofluid/energy studies, heat transfer and numerical computation in Mechanical Engineering.

Mustafa Mohamed Mundu is an Assistant Lecturer in the Department of Physical Sciences, Kampala International University. He holds a BSc (Physics, Mathematics, 2006), MSc Physics (2013), a student of PhD in Renewable Energy at Kampala International University, Uganda under the supervision of *Stephen Ndubuisi Nnamchi*. He is carrying out doctoral research on comparative study

of solar power potential, generation and transmission in different regions of Uganda. He has several publications in optical transmissions and thermal systems.

Osarue Osaruene Edosa is an Assistant Lecturer in Mechanical Engineering Department, Kampala International University, Uganda. He holds a Bachelor and a Master's degree in Mechanical Design and Production Engineering from University of Benin (2008) and University of Lagos (2014), Nigeria respectively. He is currently pursuing a PhD in Makerere University Uganda. His research interests are composites material development and characterization, Mechanical behaviour of materials and responses to deformation, Mechanical design and Manufacturing.

Article History
Received: 17 October 2018
Accepted: 04 December 2018
Published: February 2019

Citation
Nnamchi SN, Nnamchi OA, Sangotayo EO, Mundu MM, Edosa OO. Design and fabrication of insulation testing rig. *Indian Journal of Engineering*, 2019, 16, 60-79

ABSTRACT

A three-fold design and fabrication of insulation testing rig (ITR) has been demonstrated in this research work via geometric (or architectural) design, stress design and thermal design. A pilot experiment on measurement of external and internal wall and fluid temperature essentially preceded the thermal design using a stainless steel vessel. The average wall and fluid temperature at steady state aided in evaluation of overall heat transfer coefficients. The designs were characterized by formulation of equations specific to the three cardinal areas of the designs. Subsequently, the formulated design equations were optimized to obtain an optimum and critical insulation thickness at the finned bath and dead pipe, respectively, whereas the thickness of construction material (steel sheet) was established by circumferential stress design of the ITR. The three key design parameters aforementioned strongly governed the architectural design of the ITR. The design results (dimension) were further translated into detailed engineering drawings, which aided in the smart fabrication of the ITR. The equipment is quite simple and affordable; it is useful for performance evaluation of insulating materials, in estimating the thermal conductivity of insulating materials and could be deployed as a laboratory equipment for demonstrating heat transfer in thermal systems.

Keywords: Geometric design, stress design, thermal design, fabrication and insulation testing rig.

1. INTRODUCTION

Loss prevention is of paramount interest in the process industries where materials, energy and personnel are virtually preserved for the optimum performance of the industries. Thus, waste heat is almost recovered and transported to the process line where it is needed for preheating of the feedstock and reheating of intermediate products. Hence, the transported heat is technically preserved by careful insulation of the conduits so as to minimize heat loss to the surroundings. However, well established industrial insulating materials like rock wool, fiberglass, foams, asbestos, plastics, etc are very exorbitant. Consequently, the need for sourcing local insulating materials which could effectively substitute the developed ones with a reasonable resistance to alteration in the ambient conditions becomes imperative.

According to Gregorec (2006) insulators are subjected to many incompatible substances which obviously contribute to their inefficiency; such as excessive heat or cryogenic condition, moisture, vibration, dirt, oil, and corrosive vapour, which are responsible for their early deterioration. Generally, testing the integrity of an insulating material requires measuring its resistance to current flow through it (which is analogous to thermal resistance). In the same vein, the present work considers application of thermal flux on the insulating materials to ascertain their suitability. Empirically, low insulator surface temperature implies that little heat is being transferred and vice-versa. Similar to electrical insulation testing; thermal flux which is passed through the insulating materials could be classified into three types; the capacitance heat flux, the absorption heat flux and the leakage heat flux. The capacitance heat flux is due to unsteady state heat conduction which vanishes as the temperature tends to stabilize in the insulating materials. The absorption heat flux is phenomenal as the insulator absorbs the heat and also disappears as stability is attained. The leakage heat flux is a portion of heat flux which escapes through the insulating materials to the surrounding at a low temperature. Insistently, this is thermal flux that exists beyond the unsteady state condition. Significantly, a rise in the leakage heat flux is an indication that the insulating material has deteriorated and needs to be replaced.

Practically, the sophisticated equipment for the purpose of testing new insulating materials is equally costly. Notwithstanding, the revolutionary researches on these equipment for testing the thermal insulation of materials abound in literature; such as heat flow meter (Flori et al., 2017), guarded heat flow meters (Salmon, 2001), guarded hot plate instrument (Li et al., 2012), flash diffusivity methods (McMasters et al., 2017), calibrated hot box (Lawal and Ugheoke, 2012). The accuracy and agreement among the variants of the guarded hot plate occurs at ambient temperature and large variance occurs at cryogenic or superheated conditions (Flynn et al., 2002). The excessive cost of these equipment is inevitable and unaffordable. Thus, there is an overwhelming need to develop a simple and affordable device that can perform an equivalent function. Hence, the present work is aimed at developing a finned bath which enhances the rate of transfer of thermal flux to the insulating materials; and capable of performing spatial and a time measurement of characteristics of the insulating materials. Also, the present design adopts ambient condition as the cold surface, which will guarantee the accuracy of the design results (Eithun, 2012).

Subsequently, Frawley and Kennedy (2007) introduced a hot box apparatus; which could be calibrated, guarded or combination of both (edged hot box). The test technique is ex situ in the sense that test is conducted without the interference of environmental factors. Actually, this technique presents an ideal thermal characteristic of an insulating material that is to be subjected to environmental condition (Simko et al., 1999; Abdeen Mustafa Omer, 2018). Moreover, hot box promotes radiation losses, sequel to variation in its wall temperature. The present work will adopt an in situ technique, which the test material is not excluded from the stimulus effect of the surroundings for the purposes of presenting a true or real life performance of an insulating material. The cold comportment of the hot box equipment is equivalent to the immediate surroundings of the insulation testing rig (ITR), moreover, the finned bath is to be designed to maintain high thermal flux through the insulator for the unsteady-state and steady-state performance evaluation of the insulating materials. As a matter-of-fact, developing countries have no choice than to fashion a prototype device that will fulfill the dual purpose of testing and discovering new insulating materials by designing a simple and affordable insulation testing device or rig.

Thus, the unique feature of the present design will be pivoted on; the geometric formulation of the design equations for sizing of the different components of the ITR– the finned bath and the dead pipe in Figure 2; consideration of stress on the ITR to determine the metal sheet thickness and thermal formulation of key design parameters– the insulation thickness and critical insulation thickness around the finned bath and dead pipe, respectively. The formulation of the design equations will entrench the application of derivative or gradient technique for optimizing the key design parameters and in the optimal sizing of the ITR parameters formulated with the optimum design parameters.

The cylindrical or radial test surface will be adopted due to its accuracy (98%) in measurement of thermal conductivity (Eithun, 2012). However, the finned bath surface of the ITR could be equally deployed for the measurement of thermal conductivity of walled or sheet specimens with the environment as the heat sink. Moreover, the evaluation of the heat transfer coefficients within and around the ITR, will necessitate a pilot measurement of temperature difference at the interior and exterior surfaces of a model stainless steel vessel for the ease of evaluation of the thermal properties, which will culminate in deterministic design of the ITR.

The design data (mostly the dimensions) will be translated into several drawings; the isometric, orthographic projection and sectional views for a smart fabrication of the ITR.

Besides, the ITR is intended to be flexible for testing insulating materials of different sizes such as pulverized and fibrous materials due to the advantage of elongated cylindrical testing surface.

Thus, the present work is concerned with the comprehensive design and fabrication of insulation testing rig for the purposes of discovering new local insulating materials, mostly the agricultural solid wastes on in situ basis.

2. MATERIALS AND METHOD

The research work will combine experiments and designs for the purpose of achieving the set objectives of this work. The experiment is imperative in order to establish the forced or external and natural or internal convective heat transfer coefficients, which are essential for computing the overall heat transfer coefficient and for the thermal designs of the ITR.

2.1. Experimentation

Approximately, a*2*(*liter*) stainless steel vessel was filled with a freshwater almost to the brim. Then, the lid was kept in place while the heat source was powered from a *220 V* (*13 A, 50Hz*) alternating current (AC) source to heat up the electric filament of the heat source. The heat source was maintained at temperature of *400 – 500* (^oC). External and internal measurement of temperature were observed at unsteady-state condition (prior to boiling) and steady condition (during boiling) using UNI-T (UT33C) multi-meter via a thermocouple wire. Internally, the stainless steel temperature; at its top, middle and base were recorded together with the uniformly distributed working fluid temperature. Externally, the lid temperature, the side wall temperature; at its middle and base were measured. Also, observation were made among the bulk air temperature, $T_{air,\infty}$, surrounding air temperature, T_{air} and the external wall temperature. The average external wall temperature and surrounding air temperature was useful for evaluating the forced heat transfer coefficient and other thermal properties of the working fluid (air). Also, similar observation was internally made in order to estimate the free or natural heat transfer coefficient and other relevant thermal properties of working fluid (freshwater). The measurement was repeated for three times and the average temperature values employed in carrying out the thermal design of the insulation testing rig. The experimental results for air-wall and wall-freshwater are recorded in Tables 2 and 3, respectively. Substantially, the experimental set up is shown in Figure 1.

1 a. Internal temperature measurement

1 b. External temperature measurement

Figure 1 The pilot experimental setup

2.2. Design formulation

The geometric and thermal formulation of design equations is considered premium in the design of the insulation testing rig. These equations are to be deployed in optimization and computation of the essential dimension of the insulation testing rig and in realization of the supporting engineering drawings (the sectional and isometric views of the insulation testing rig) essential for the fabrication of the ITR.

2.2.1. Geometric Design of the insulation testing rig

Considering the geometric design of the dead pipe (dp) and finned bath (fb) in Figure 2, which isa schematic representation of the insulation testing rig (ITR).

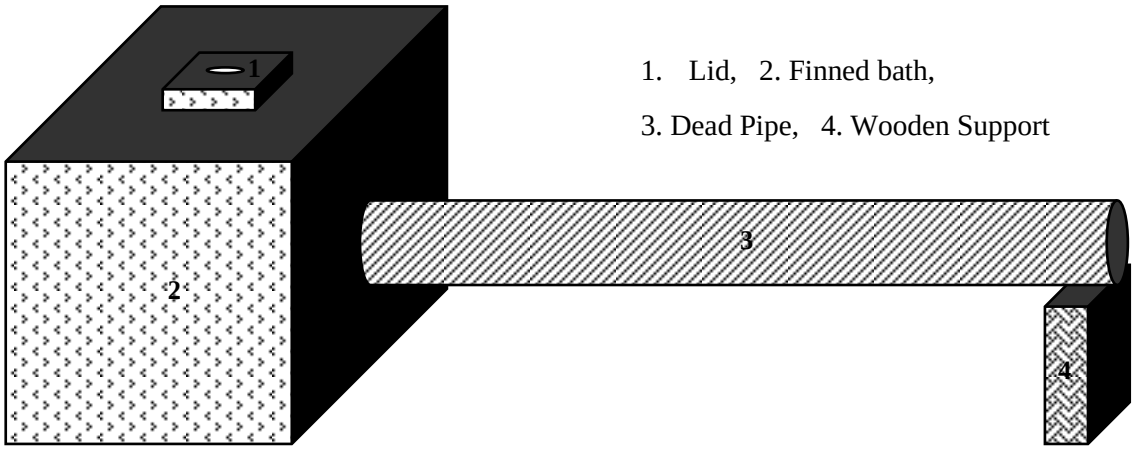

1. Lid, 2. Finned bath,
3. Dead Pipe, 4. Wooden Support

Figure 2 Schematic representation of insulation testing rig (ITR) with the box designating the finned bath and the cylinder depicting the dead pipe

2.2.1.1. Sizing of the dead pipe:

The input data for sizing of the dead pipe are;the length, l_{dp} (m) and outer diameter, OD_{dp} (m), respectively;

The inner diameter of the dead pipe, ID_{dp}in Equation 1 is defined as follows:

$$\begin{aligned} & ID_{dp} = OD_{dp} - 2\delta_s \\ & \Rightarrow 2r_i = 2r_o - 2\delta_s \quad ; \; ID_{dp} = 2r_i \; ; \; OD_{dp} = 2r_o \; ; \\ & \Rightarrow r_i = r_o - \delta_s \quad (m) \end{aligned} \tag{1}$$

where δ_s (m) is the thickness of construction material (mild steelsheet, s), r_i and r_o is the inner (i)and outer (o)radius of the dead pipe, respectively.

Alternatively, the inner radius of the dead pipe, r_i in Equation 2 could be derived as

$$r_i = \frac{ID_{dp}}{2} = \frac{OD_{dp} - 2\delta_s}{2} = r_o - \delta_s \quad (m) \tag{2}$$

Thus, the available curved surface area, $A_{dp}$of the dead pipefor exchanging heat with the surroundings is given in Equation 3 as

$$A_{dp} = 2\pi r_o l_{i,dp} + \pi r_o^2 = \pi r_o \left(2l_{i,dp} + r_o\right) = \pi \left(\frac{OD_{dp}}{2}\right)\left(2l_{i,dp} + \frac{OD_{dp}}{2}\right) \quad (m^2) \tag{3}$$

where $l_{i,dp}$ is the inner length of the of the dead pipe occupied by the fluid.

The outer length of the insulator on the dead pipe, $l_{o,ins}$ is expressed in Equation 4 as

$$l_{o,ins} = l_{i,dp} - \delta_{ins} + \delta r^*_{ins,dp} \quad (m); \; l_{i,ins} = l_{o,ins} - \delta_s \quad (m); \; l_{o,dp} = l_{i,dp} + \delta_s \quad (m) \tag{4}$$

where $\delta_{ins}\left(\delta_{ins}^{*}\right)$is the optimum insulation thickness around the finned bath and $\delta r_{ins,dp}\left(\delta r_{ins,dp}^{*}\right)$ is the critical insulation thickness around the dead pipe.

The actual volume of fluid in the dead pipe, V_{dp} for fully developed profile is formulated by substituting Equation 1 or 2 into Equation 5

$$V_{dp} = \pi r_i^2 l_{dp} = \pi\left(r_o - \delta_s\right)^2\left(l_{dp}\right) \quad \left(m^3\right) \tag{5}$$

2.2.2.2. Sizing of the finned bath:

The basic input data necessary for determining the unit cross sectional area (CSA) and full dimension of the finned bathare the length and height of the heater or heating source, l_{hs} and ht_{hs}, respectively, which is fixed by the dimension of heat source.

The interior volume of the finned bath is made up of a free board space (*fbs*), $V_{fbs}\left(m^3\right)$ and fluid space (*fs*), V_{fs} which is given in Equation 6

$$V_{i,B} = V_{fbs} + V_{fs} \quad \left(m^3\right) \tag{6}$$

where the volume of fluid in the finned bath is related to the volume of fluid in the dead pipein Equation 7 as

$$V_{fs} = n\,V_{dp} = n\,\pi\,r_i^2\left(l_{dp}\right) = n\,\pi\left(r_o - \delta_s\right)^2\left(l_{dp}\right) \quad \left(m^3\right) \tag{7}$$

where *n* is a multiplierfor scaling up the insulation testing rig capacity.

Therefore the interior volume of the finned bath, $V_{i,B}$in Equation 8 becomes

$$V_{i,B} = V_{fbs} + n\,V_{dp} \quad \left(m^3\right) \tag{8}$$

and forsafeoperation of the finned bath, the free board space is set to be one-third of the fluid space in Equation 9

$$V_{fbs} = \frac{V_{fs}}{3} = \frac{nV_{dp}}{3} = \frac{n\pi\left(r_o - \delta_s\right)^2\left(l_{dp}\right)}{3} \quad \left(m^3\right) \tag{9}$$

Thus, the interior volume of the finned bath, $V_{i,B}$ in Equation10 becomes

$$V_{i,B} = \frac{nV_{dp}}{3} + n\,V_{dp} = \frac{4}{3}n\,V_{dp} = \frac{4}{3}n\,\pi\left(r_o - \delta_s\right)^2\left(l_{dp}\right) \quad \left(m^3\right) \tag{10}$$

and the interior volume of the insulation testing rig, $V_{i,ITR}$ in Equation 11 is given as

$$V_{i,ITR} = V_{i,B} + V_{dp} = \frac{4}{3}n\,\pi\left(r_o - \delta_s\right)^2\left(l_{dp}\right) + \pi\left(r_o - \delta_s\right)^2\left(l_{dp}\right)$$
$$V_{i,ITR} = \pi\left(r_o - \delta_s\right)^2\left(l_{dp}\right)\left(\frac{4}{3}n + 1\right) \quad \left(m^3\right) \tag{11}$$

The interior (or inner) cross sectional area of the finned bath, $A_{i,B}$is conformed to the base of the heat source (a regular square geometry), which is expressed in Equation 12 as

$$A_{i,B} = (l_{hs})^2 \qquad (m^2) \tag{12}$$

The height of the free board space, ht_{fbs} in Equation 13is ratio of its interior volume to the surface area of the heat source;

$$ht_{fbs} = \frac{V_{fbs}}{A_{fbs}} = \frac{V_{fbs}}{A_{i,B}} = \frac{n\,\pi(r_o - \delta_s)^2(l_{dp})}{3A_{i,B}} \qquad (m) \tag{13}$$

Similarly, the height of the fluid space, ht_{fs} in Equation 14 is given as

$$ht_{fs} = \frac{V_{fs}}{A_{fs}} = \frac{V_{fs}}{A_{i,B}} = \frac{n\,\pi(r_o - \delta_s)^2(l_{dp})}{A_{i,B}} \qquad (m) \tag{14}$$

The interior height of the finned bath, $ht_{i,B}$ in Equation 15 is obtained by summation of the two heights; ht_{fbs} and ht_{fs}, which culminates into

$$ht_{i,B} = ht_{fbs} + ht_{fs_s} = \frac{n\,\pi(r_o - \delta_s)^2 l_{dp}}{3A_{i,B}} + \frac{n\pi(r_o - \delta_s)^2 l_{dp}}{A_{i,B}}$$

$$ht_{i,B} = \frac{4}{3}\frac{n\,\pi(r_o - \delta_s)^2 l_{dp}}{A_{i,B}} \qquad (m) \tag{15}$$

The outer height of the finned bath, $ht_{o,B}$ in Equation 16is given as

$$ht_{o,B} = ht_{i,B} + ht_{hs} + 3\delta_s + \delta_{ins} \qquad (m) \tag{16}$$

where δ_{ins} (*m*) is the thickness of the insulator to be determined by thermal designs (or balance) .

The inner and outer breadth of the finned bath, $w_{i,B}$ and $w_{o,B}$, respectively in Equation 17 is given as

$$w_{i,B} = l_{hs} \qquad (m)$$

And $w_{o,B} \approx w_{i,B} + 2(2\delta_s + \delta_{ins}) = w_{i,B} + 4\delta_s + 2\delta_{ins} = l_{hs} + 4\delta_s + 2\delta_{ins} \qquad (m)$ (17)

Then, the peripheral area of the finned bath, $A_{o,B}$ in Equation 18 is computed as follows:

$$A_{o,B} = w_{o,B}^2 + 4ht_{o,B}\,w_{o,B} = (l_{hs} + 4\delta_s + 2\delta_{ins})^2 + 4(ht_{i,B} + 3\delta_s + ht_{hs} + \delta_{ins})(l_{hs} + 4\delta_s + 2\delta_{ins}) \qquad (m^2) \tag{18}$$

The inner and outer dimension of the lid, $w_{i,lid}$ and $w_{o,lib}$ of the finned bath in Equation 19 is specified as

$$w_{i,lid} = \frac{w_{i,B}}{3} \quad (m) \tag{19}$$

And $w_{o,lid} = w_{i,lid} + 2\delta_s = \frac{w_{i,B}}{3} + 2\delta_s \quad (m)$, respectively.

The height of the lid, ht_{lid} in Equation 20 is specified as

$$ht_{lid} = 0.01 + 2\delta_s + \delta_{ins} \quad (m) \tag{20}$$

The outer and inner breath of the handle, $w_{o,handle}$ and $w_{i,handle}$ in Equation 21 is specified as

$$w_{o,handle} = \frac{w_{i,B}}{6} = \frac{l_{hs}}{6} \ (m) \text{ and} \tag{21}$$

$$w_{i,handle} = \frac{w_{i,B}}{6} - 2\delta_s = \frac{l_{hs}}{6} - 2\delta_s \quad (m), \text{ respectively.}$$

The height of the handle, ht_{handle} in Equation 22 is specified as

$$ht_{handle} = 0.02 + \delta_s \quad (m) \tag{22}$$

The breath of the feeder, w_{feeder} in Equation 23 is specified as

$$w_{feeder} = \frac{w_{i,B}}{3} - 2\delta_s = \frac{l_{hs}}{3} - 2\delta \quad (m) \tag{23}$$

The height of the feeder, ht_{feeder} in Equation 24 is specified as

$$ht_{feeder} = 0.02 + 2\delta_s + \delta_{ins} \quad (m) \tag{24}$$

2.2.3. Stress Consideration in the Insulation Testing Rig

The circumferential thermal stress (Hoop stress), σ_c and the maximum thermal stress, $\sigma_{\max}$ in thin wall cylindrical shapes (Engineering ToolBox, 2018; Brown, 2005) is given in Equation 25 as

$$\sigma_c = \left[\frac{P_i r_i^2 - P_o r_o^2}{r_o^2 - r_i^2}\right] - \left[\frac{r_i^2 r_o^2 (P_o - P_i)}{r^2\left(r_o^2 - r_i^2\right)}\right] \ (MPa); \ \sigma_{\max} = \left[\frac{P_i r_i^2 - P_o r_o^2}{r_o^2 - r_i^2}\right] - \left[\frac{r_i^2 r_o^2 (P_o - P_i)}{r_i^2\left(r_o^2 - r_i^2\right)}\right] \ (MPa) \tag{25}$$

where r_i is the inner radius of the cylinder, r_o is the outer radius of cylinder, P_i is the internal (vessel) pressure, P_o is the external (atmospheric) pressure.

By applying the equivalent hydraulic (H) diameter (D), $D_H\left\{D_{i,H}, D_{o,H}\right\}$ for the square cross section of theITR, D_H is given in Equation 26 as

$$D_{i,H} = \frac{4w_{i,B}^2}{2\left(2w_{i,B}\right)} = w_{i,B} = l_{hs} \quad (m); \; D_{o,H} = \frac{4w_{o,B}}{2\left(2w_{o,B}\right)} = w_{o,B} \quad (m) \tag{26}$$

Equation 25is adapted to square cross section in Equation 27 as follows:

$$\sigma_c = \left(\frac{P_i w_{i,B}^2 - P_o w_{o,B}^2}{w_{o,B}^2 - w_{i,B}^2} - \frac{w_{i,B}^2 w_{o,B}^2 \left(P_o - P_i\right)}{w_B^2 \left(w_{o,B}^2 - w_{i,B}^2\right)} \right) \quad (MPa);$$

$$\sigma_{\max} = \left(\frac{P_i w_{i,B}^2 - P_o w_{o,B}^2}{w_{o,B}^2 - w_{i,B}^2} - \frac{w_{o,B}^2 \left(P_o - P_i\right)}{w_{o,B}^2 - w_{i,B}^2} \right) \quad (MPa) \;\; \exists \;\; w_B^2 = w_{i,B}^2 \tag{27}$$

Equation 28 gives the internal pressure, P_i which is related to the external pressure, P_o as follows:

$$P_i = n'' P_o \quad \left(MPa\right); \quad \exists \quad P_i > P_o \tag{28}$$

where n'' is a constant of proportionality between P_i and P_o .

Thus, substituting Equation 28 into 27 gives Equation 29 a modified form of Equation 27 as follows:

$$\sigma_{\max} = P_o \left(\frac{n'' w_{i,B}^2 - w_{o,B}^2}{w_{o,B}^2 - w_{i,B}^2} - \frac{w_{o,B}^2 \left(1 - n''\right)}{w_{o,B}^2 - w_{i,B}^2} \right) \quad (MPa) \; ;\exists$$

$$\Rightarrow w_{o,B} = \left[\frac{w_{i,B}^2 \left(n'' + \frac{\sigma_{\max}}{P_o} \right)}{n'' - 2 + \frac{\sigma_{\max}}{P_o}} \right]^{\frac{1}{2}} \quad (m) \tag{29}$$

The thickness of the construction material (steel sheet), δ_s in Equation 30 is given as

$$\delta_s = 0.25 \left(w_{o,B} - w_{i,B} - 2\delta_{ins} \right) \quad (m); \tag{30}$$

2.2.4. Thermal design of the Insulation Testing Rig

The heat transfer between the heat source and heat sink (the surroundings) is designed such that minimal heat loss is concede or transferred to the surroundings. Principally, the heat supplied from the heat source does not produces any work (since there is no moving boundary).Thermodynamically, the heat supplied only raises the internal energy of the working fluid (freshwater). The

thermal gradient from the heat source to the heat sink is carefully articulated in Figure 3 in order to account for the effect of the individual resistance sequel to conduction and convection current (heat fluxes).

The thermal design will be carried out on the dead pipe and finned bath in order to determine the critical parameters; the insulation thickness of the dead pipe and finned bath. Figures 3 and 4 represent the thermal gradient at the finned bath and dead pipe, respectively.

The design consideration in Figure 3 centers on calculation of insulation thickness, δ_{ins}. This is to be realized by computing heat transferred between the hot and cold fluids in Figure 3a for different conditions; insulation testing rigs with and without insulating materials.

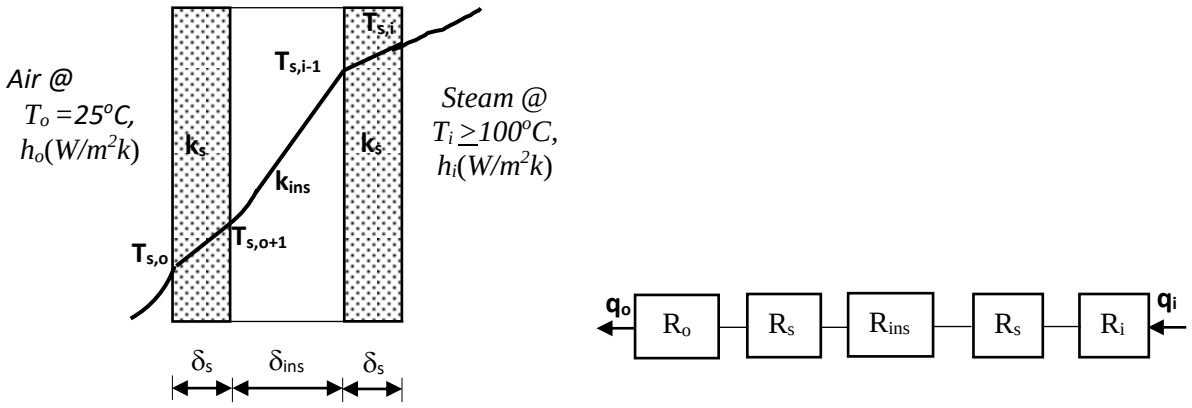

(a) Thermal gradient **(b)** Thermal resistance of a composite material

Figure 3 Thermal gradient across the bath of the insulation testing rig (ITR)

According to Rajput (2007) certain amount of heat has to be conceded to the surroundings from the finned bath compartment. For the purposes of design, about 75 or more percent (%) of heat generated is to be conserved. Thus, Equation 31 represents the heat transfer across the cold and hot fluid without an insulator, Q , which is modelled by Oko and Nnamchi (2012) as

$$Q = U'_L A'_{o,B} \Delta T \qquad (W) \qquad 31$$

where U'_L is the overall heat transfer coefficient which is defined in Equation 32as

$$U'_L = \frac{1}{R_L} = \frac{1}{\frac{1}{h_o} + \frac{\delta_S}{k_S} + \frac{1}{h_i}} \qquad \left(W/m^2K\right) \qquad 32$$

where $A'_{o,B}$ is the overall surface area of the finned bath available for heat transfer without an insulator is expressed in Equation 33

$$A'_{o,B} = \left(w_{i,B} + 2\delta_s\right)^2 + 4\left(ht_{i,B} + 2\delta_s + ht_{hs}\right)\left(w_{i,B} + 2\delta_s\right)$$
$$A'_{o,B} = \left(l_{hs} + 2\delta_s\right)^2 + 4\left(ht_{i,B} + 2\delta_s + ht_{hs}\right)\left(l_{hs} + 2\delta_s\right) \qquad \left(m^2\right) \qquad 33$$

where ΔT is the temperature difference in Equation 34

$$\Delta T = T_i - T_o \qquad (K) \qquad 34$$

Conversely, Equation 35 modelsthe heat transfer, Q_{ins} across the cold and hot fluid with an insulator

$$Q_{ins} = U_L A_{o,B} \Delta T \qquad (W) \tag{35}$$

where U_L is the overall heat transfer coefficient in Equation 36is defined as

$$U_L = \frac{1}{R_L} = \frac{1}{\frac{1}{h_o} + \frac{2\delta_s}{k_s} + \frac{\delta_{ins}}{k_{ins}} + \frac{1}{h_i}} \qquad \left(W/m^2K\right) \tag{36}$$

where $A_{o,B}$ is the surface area of the finned bath available for heat transfer, which is geometrically determined in Equation 18.

Thus, to achieve high reduction in heat loss, Rajput (2007) suggests that the rate of heat transfer with an insulator in place, Q_{ins} should be balanced by the product of fraction of heat loss, n' and the rate of heat transfer without an insulator in place, Q_{ins} which is expressed in Equation 37 as follows:

$$Q_{ins} \approx n' Q; \quad n' > 0.1 \tag{37}$$

Substituting Equations 18, 31– 36 into Equation 37 yields Equation 38, a thermal function, $f(\delta_{ins})$ as

$$\begin{aligned} f(\delta_{ins}) = &\left(\frac{1}{\frac{1}{h_i} + \frac{2\delta_s}{k_s} + \frac{\delta_{ins}}{k_{ins}} + \frac{1}{h_o}}\right)\left[\left(l_{hs}+4\delta_s+2\delta_{ins}\right)^2 + 4\left(ht_{i,B} + 3\delta_s + ht_{hs} + \delta_{ins}\right)\left(l_{hs}+4\delta_s+2\delta_{ins}\right)\right](T_i - T_o) \\ &- n'\left(\frac{1}{\frac{1}{h_i} + \frac{\delta_s}{k_s} + \frac{1}{h_o}}\right)\left[\left(l_{hs}+2\delta_s\right)^2 + 4\left(ht_{i,B} + 2\delta_s + ht_{hs}\right)\left(l_{hs}+2\delta_s\right)\right](T_i - T_o) = 0 \qquad (W) \end{aligned} \tag{38}$$

The present work suggests that the optimum insulation thickness of the finned bath, δ_{ins} should be determined by differentiating $f(\delta_{ins})$ in Equation 38 with respect to δ_{ins} and equating the resulting derivative to zero results in Equation 39

$$\begin{aligned} \frac{df(\delta_{ins})}{d\delta_{ins}} = &\left(\frac{1}{h_i} + \frac{\delta_s}{k_s} + \frac{1}{h_o}\right)\left[4\left(l_{hs} + 4\delta_s + 2\delta_{ins}\right) + 4\left(l_{hs} + 4\delta_s + 2\delta_{ins}\right) + 8\left(ht_{i,B} + ht_{hs} + 3\delta_s + \delta_{ins}\right)\right] \\ &- \frac{n'}{k_{ins}}\left[\left(l_{hs} + 2\delta_s\right)^2 + 4\left(ht_{i,B} + ht_{hs} + 2\delta_s\right)\left(l_{hs} + 2\delta_s\right)\right] = 0 \qquad \left(m^3/W\right) \end{aligned} \tag{39}$$

Simplifying Equation 39, gives the optimum values of δ_{ins} (δ^*_{ins}) in Equation 40as

$$\delta^*_{ins} = \frac{1}{24\left(\frac{1}{h_i} + \frac{\delta_s}{k_s} + \frac{1}{h_o}\right)}\left\{\begin{aligned} &\frac{n'}{k_{ins}}\left[\left(l_{hs} + 2\delta_s\right)^2 + 4\left(ht_{i,B} + ht_{hs} + 2\delta_s\right)\left(l_{hs} + 2\delta_s\right)\right] \\ &-8\left(\frac{1}{h_i} + \frac{\delta_s}{k_s} + \frac{1}{h_o}\right)\left[\left(l_{hs} + 4\delta_s\right) + \left(ht_{i,B} + ht_{hs} + 3\delta_s\right)\right] \end{aligned}\right\} \quad (m) \tag{40}$$

Carrying out a similar heat transfer analysis around the dead pipe. Figure 4 shows the thermal gradient and resistance across the dead pipe.

The critical radius of insulation thickness that causes sudden decrease or change in a progressive heat flux is obtained by establishing the thermal flux from hot to cold fluid in Equation 41 as

$$T_i - T_o = \frac{Q}{2\pi l_{ins}}\left[\frac{1}{r_i h_i, c} + \frac{\ln\left(r_{o,s}/r_{i,s}\right)}{k_s} + \frac{\ln\left(r_{ins}/r_{o,s}\right)}{k_{ins}} + \frac{1}{r_{ins}h_{o,c}}\right] \qquad (K) \qquad 41$$

where $r_{o,s}$ is the outer radius of the dead pipe, which is defined in Equation 42 as

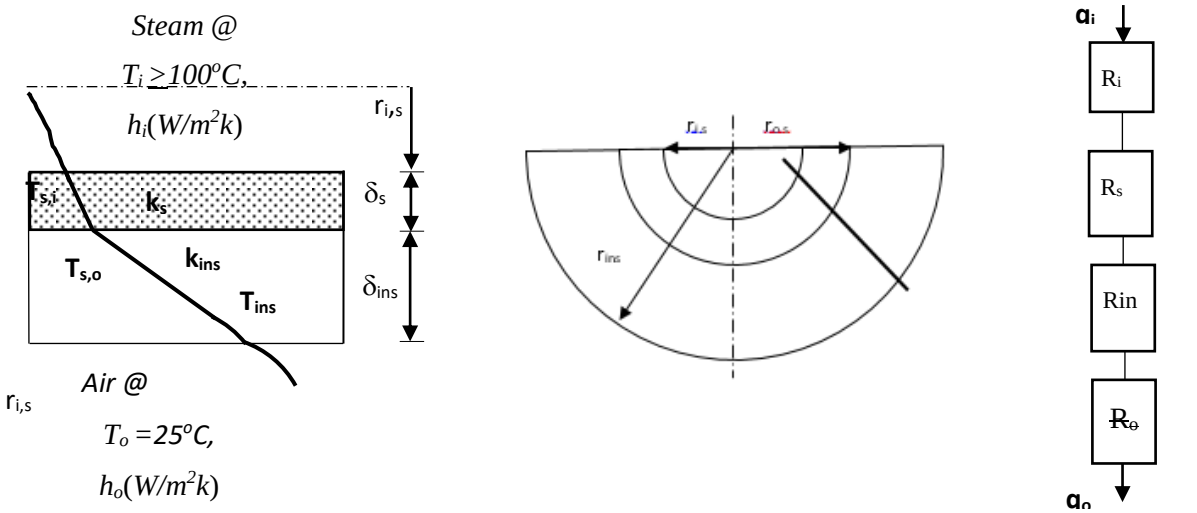

(a) Lateral thermal gradient **(b)** Semicircular thermal gradient **(c)** Thermal resistance of different materials

Figure 4 Thermal gradient across the finned pipe of ITR

$$r_{o,s} = r_{i,s} + \delta_s \qquad (m) \qquad 42$$

and the radius of insulation, r_{ins} is given in Equation 43as

$$r_{ins} = r_{o,s} + \delta_{ins} \qquad (m) \qquad 43$$

Equation 44describes the overall resistance to heat transfer, $R_L$as

$$R_L = \frac{1}{2\pi l_{ins}}\left[\frac{1}{r_i h_{i,c}} + \frac{\ln\left(r_{o,s}/r_{i,s}\right)}{k_s} + \frac{\ln\left(r_{ins}/r_{o,s}\right)}{k_{ins}} + \frac{1}{r_{ins}h_{o,c}}\right] \qquad \left(\frac{mK}{W}\right) \qquad 44$$

The optimum insulation thickness, r^*_{ins} in Equation 45is obtained by differentiating R_L with respect to (wrt) the insulation radius, r_{ins} as follows:

$$\frac{1}{k_{ins}\, r_{ins}} - \frac{1}{r_{ins}^{2}\, h_{o,cylinder}} = 0 \quad \Rightarrow r_{ins}^{*} = \frac{k_{ins}}{h_{o,cylinder}} \approx \delta_{ins,dp}^{*} \qquad (m) \qquad 45$$

2.2.5. Determination of Convective Heat Transfer Coefficients

The convective heat transfer coefficients on the interior and exterior of the finned bath is typical of that on vertical plane wall, which is composed of inner and outer films, $h_{i,bath}$ .and $h_{o,bath}$, respectively. The vital convective heat transfer coefficient for determining the critical insulation thickness of thedead pipe is the external film coefficient, $h_{o,cylinder}$. The convective heat transfer coefficients are to be evaluated using established empirical correlation in the literature as applied to vertical plane wall and horizontal cylinder.

For the finned bath the internal (or natural) convective heat transfer coefficient, $h_{i,bath}$ Equation 46 is given in Nnamchi et al. (2018) as

$$h_{i,bath} \approx \frac{k}{\left(ht_{fbs} + ht_{fs}\, f_s\right)}\left\{0.825 + \frac{0.387 Ra_i^{1/6}}{\left[1+(0.492/\Pr)^{9/16}\right]^{8/27}}\right\}^{2} \quad for\ 10^{-1} < Ra_i < 10^{12},$$

$$Ra_i = Gr_{ht_{fbs}+ht_{fs}} \Pr;\quad Gr_{ht_{fbs}+ht_{fs}} = \frac{g\left(ht_{fbs} + ht_{fs}\, f_s\right)^{3} \beta\,(T_s - T_\infty)}{\mu^2/\rho^2},\ \Pr = \frac{\mu_{water}\, cp_{water}}{k_{water}} \qquad (46)$$

where $k\,(W/mK)$ is the thermal conductivity of the working fluid (freshwater), $Ra(-)$ is Rayleigh's dimensionless number, $\Pr(-)$ is Prandtl number, g is the gravitational constant, $\beta(1/K)$ is the temperature coefficient, $T_S(K)$ is the inner wall temperature, $T_\infty(K)$ is the internal bulk fluid temperature, $\mu(kg/m/s)$ is the dynamic viscosity and ρ is the density of the fluid in the ITR.

Also, for the finned bath, the external (or forced) convective heat transfer coefficient, h_o (Equation 47) is defined in Nnamchi et al. (2018) as

$$h_{o,B} \approx 0.664 \frac{k}{\left(ht_{fbs} + ht_{fs}\right)} \mathrm{Re}_{o,B}^{1/2} \Pr^{1/3} \quad for\ \mathrm{Re}_{o,B} < 5\times10^{5}\ ;$$

$$\mathrm{Re}_{o,B} = \rho u \left(ht_{fbs} + ht_{fs}\right) \Big/ \mu;\quad \Pr = \mu_{air}\, cp_{air} / k_{air}\,; \qquad (47)$$

or

$$h_{o,B} \approx 0.036 \frac{k}{\left(ht_{fbs} + ht_{fs}\right)} \mathrm{Re}^{4/5} \Pr^{1/3} \quad \exists \quad \mathrm{Re}_{ht_{fbs}+ht_{fs}} > 5\times10^{5}$$

where $\mathrm{Re}_{o,B}(-)$ is the Reynolds number.

For the dead pipe the external convective heat transfer coefficient over a horizontal cylinder, $h_{o,c}$ in Equation 48 is given as (Skočilasová, 2018; Sistemas, 2018).

$$h_{o,cylinder} \approx \frac{k}{OD_{cylinder}}\left[0.193\,\mathrm{Re}_{OD_{cylinder}}^{0.618}\,\mathrm{Pr}^{1/3}\right] \quad \exists \quad \mathrm{Pr} \geq 0.70,\ \ 4000 \leq \mathrm{Re}_{OD_{cylinder}} \leq 40000 \qquad (48)$$

3. DISCUSSION AND RESULTS

The output of the designs of the insulation testing rig and the discussion thereon is as follows:

3.1. Design Input Data

Table 1 represents the general input or primary data to the design equations (Equations 1 – 48). Table 1 is embodiment of physical constants and measurement on the dimension of the heat source which governed the cross sectional area of the ITR. Table 2 proffers the thermal properties of the interior working fluid (freshwater) and the dimensionless numbers necessary for prescribing the free or natural convection between the bulk fluid and the interior walls of the finned bath. Similarly, Table 3 summaries the thermophysical properties of the external working fluid (air) and all the essential dimensionless numbers which describe the forced convection around the ITR. In addition, Tables 1 – 3 are not the major results but serve as input data for the designs.

Table 1 General input data

S#	Parameter	Unit	value
1.	Length of the heat source, $l_{hs} = w_{iB}$	(m)	0.24000
2.	Height of the hot source, ht_{hs}	(m)	0.08000
3.	Size of the dead pipe, l_{dp}	(m)	0.97536
4.	Scaling factor, n	(-)	4.00000
5.	Heat loss factor, n′	(-)	0.21599
6.	Pressure proportionality constant, n′′	(-)	2.00000
7.	Thermal conductivity of the insulator, k_{ins}	($Wm^{-1}\,K^{-1}$)	0.28250
8.	Thermal conductivity of the steel sheet, k_s	($Wm^{-1}\,K^{-1}$)	36.03947
9.	The outer diameter, *OD* of the dead pipe	(m)	0.07000
10.	Gravitational constant, g	($m\,s^{-2}$)	9.81000
11.	The external (atmospheric) pressure, P_o	(MPa)	0.101325
12.	Maximum allowable pressure, σ_{max}	(MPa)	0.266061

Table 2 Properties of freshwaterat average inner wall and freshwater temperature of 380.15 and383.15 (K), respectively

S#	Parameter	Unit	Equation	value
1.	Mean temperature, $\overline{T}$	(K)		381.65000
2.	Temperature coefficient, β	(K^{-1})		0.00262
3.	Density, ρ	($kg\,m^{-3}$)	$\rho = 754.3079871 + 1.88132843\overline{T} - 0.0035831\overline{T}^{2}$	950.41438
4.	Viscosity, μ	($kg\,m^{-1}\,s^{-1}$)	$\mu = 1460398670\ \ 76.91\,\overline{T}^{-5.74}$	0.00022
5.	Heat capacity, cp	($kJ\,kg^{-1}\,K^{-1}$)	$cp = 5.476 - 0.008178\ \overline{T} + 0.000013\ \overline{T}^{2}$	4.24869
6.	Thermal conductivity, k	($Wm^{-1}\,K^{-1}$)	$k = \ 0.0223\ \overline{T}^{0.5802}$	0.70176
7.	Prandtl, Pr	(-)	$Pr = \ 2391.7\ exp\left(-0.02\,\overline{T}\right)$	1.15808
8.	Grashoff, Gr	(-)	Equation46	3.75842×10^{10}

9.	Rayleigh, Ra	(-)	Equation 46	4.35254×10^{10}

Table 3 Properties of air at average outer wall and surrounding air temperature of 311.15 and 377.25 (K), respectively

S#	Parameter	Unit	Equation	value
1.	Mean temperature, $\overline{T}$	(K)		344.15000
2.	Temperature coefficient, β	(K^{-1})		0.00275
3.	Density, ρ	(kg m^{-3})	$\rho = 2.1313 - 0.003\ \overline{T}$	1.09885
4.	Viscosity, m	(kg m^{-1} s^{-1})	$\mu = 1.03\times10^{-6} + 7\times10^{-8}\,\overline{T} - 4\times10^{-11}\,\overline{T}^{\,2}$	2.03829×10^{-5}
5.	Heat capacity, cp	(kJ kg^{-1} K^{-1})	$cp = 2.1313 - 0.003\ \overline{T}$	1.01061
6.	Thermal conductivity, k	(Wm^{-1} K^{-1})	$k = 0.0121\exp\left(0.0025\ \overline{T}\right)$	0.02860
7.	Air speed, u	(m s^{-1})		2.00000
8.	Prandtl, Pr	(-)	Equations 46&47	0.72012
9.	Reynolds, Re	(-)	Equation 47	3.21510×10^{4}

3.2. Results

The key results are tabulated in Tables 4 and 5. The film coefficient computed with the information in Tables 2 and 3 for freshwater gave convective heat transfer coefficient of *1011.17 W/m²*K and that for air was *17.39488* and *12.48751 W/m²K* for air around the finned bath and dead pipe, respectively. The results are in good agreement with those stipulated in the literature (Wikipedia, 2018), which ranges from *500 – 10000 (W/m²K)* and *10 – 100 (W/m²K)* for freshwater and air, respectively. Basically, the major design results are the dimension of the insulation testing rig and the convective heat transfer coefficients of the working fluids (air and freshwater). These results are summarised in Tables 4 and 5.

Table 4 Design output data (thermal parameters)

S#	Parameter	Unit	value
1.	The natural convective transfer coefficient in the finned bath, h_i (freshwater)	(kW m^{-2} K^{-1})	1.01117
2.	The forced convective transfer coefficient around the finned bath, h_o (air)	(W m^{-2} K^{-1})	12.48751
3.	The forced convective transfer coefficient around the dead pipe, $h_{o,cylinder}$ (air)	(W m^{-2} K^{-1})	17.39488
4.	Overall resistance to heat transfer across the finned bath, R_L (without insulation)	(m^2 K W^{-1})	0.08112
5.	Overall resistance to heat transfer across the finned bath, R_L (with insulation)	(m^2 K W^{-1})	0.32920
6.	Overall heat transfer coefficient across the finned bath, R_L (without insulation)	(W m^{-2} K^{-1})	12.32681
7.	Overall resistance to heat transfer across the finned bath, R_L (with insulation)	(W m^{-2} K^{-1})	3.03769

Table 5 Design output data (dimension)

S#	Dimension	Unit	value
1.	The peripheral of the dead pipe, A_{dp}	(m^2)	0.21424

2.	The volume of fluid in the dead pipe for fully developed profile, is, V_{dp}	(m^3)	0.00334
3.	The volume of fluid in the finned bath, V_{fs}	(m^3)	0.01288
4.	The interior volume of the finned bath, $V_{T,B}$ (with insulation)	(m^3)	0.01718
5.	The interior volume of the insulation testing rig, $V_{i,TR}$	(m^3)	0.02040
6.	The interior (or inner) cross sectional area of the bath, $A_{i,B}$	(m^2)	0.05760
7.	The radius of the dead pipe, r_i	(m)	0.03302
8.	Height of free board space, ht_{fbs}	(m)	0.07455
9.	Height of fluid space, ht_{fs}	(m)	0.22364
10.	The inner height of bath, $ht_{i,B}$	(m)	0.29819
11.	The outer height of the bath, $ht_{o,B}$	(m)	0.41945
12.	The outer breadth of the bath, $w_{o,B}$	(m)	0.31855
13.	Insulation thickness around the finned bath, δ_{ins}	(m)	0.03530
14.	Insulation thickness around the dead pipe, δ^*_{ins},dp	(m)	0.01624
15.	The outer length of insulation, $l_{o,ins}$	(m)	0.95630
16.	The thickness of construction material (steel sheet), δ_s	(m)	0.00198
17.	The inner breath of the finned bath, $w_{i,B}$	(m)	0.24000
18.	The inner breath of the lid, $w_{i,lid}$	(m)	0.08000
19.	The outer breath of the lid,, $w_{o,lid}$	(m)	0.08397
20.	The height of the lid, ht_{lid}	(m)	0.04927
21.	The inner breath of the handle, $w_{i,handle}$	(m)	0.03603
22.	The outer breath of the handle, $w_{o,handle}$	(m)	0.04000
23.	The height of the handle, ht_{handle}	(m)	0.02198
24.	The breadth of the feeder, w_{feeder}	(m)	0.07603
25.	The height of the feeder, ht_{feeder}	(m)	0.05927

3.3. Discussion

The major design parameters; the thickness of the steel sheet for the fabrication of the ITR is defined by Equations 29 and 30. The results show that increasing the circumferential stress (Hoop stress)mostly increases the thickness of the steel sheet; increasing the insulation thickness partly decreases the thickness of the steel sheet and increasing the difference between the outer and inner breath of the ITR is compensated with an increment in the steel sheet thickness ($\delta_S = 0.00198 \quad (m)$ in Table 5). The maximum Hoop stress for the thin walled vessels based on the design information is 0.266061 MPa (in Table 1) which is more than twice the atmospheric pressure. Also, Equation 40 presents the optimum insulation thickness around the finned bath as function of product of overall heat transfer coefficient without insulating material and the differential characteristic volume per unit conductance with insulating material and without insulating material ($\delta^*_{ins} = 0.0353 \quad (m)$ in Table 5).

Equation 45 expresses the critical insulation thickness around the dead pipe as the ratio of thermal conductivity of the insulating material to convective heat transfer coefficient around the dead pipe ($\delta^*_{ins,dp} = 0.01624 \ (\mathrm{m})$ in Table 5).

The thickness of the steel sheet, the insulation thickness around the finned bath and the dead pipe governed the dimension of the rest of the design parameters in Table 5, especially; the architectural design of the ITR.

The design characteristic dimension gave rise to Figures 5 – 8, the isometric, orthographic, front section and plan section of the ITR, respectively. These drawings are essential for fabrication of the physical system in Figure 9.

Essentially, the fabricated ITR could serve multi-purpose functions; could be employed for performance evaluation of existing insulating materials, discovering of new insulating materials and could equally function as laboratory equipment for demonstrating heat transfer principles.

The material specification for ITR was based on their thermal properties and resistance to corrosion; the galvanized steel was chosen for the lining of the ITR to withstand thermal stress and corrosion effects for long use and mild steel was selected for the outer cover because it is not subjected to high thermal stress, which alleviates the cost of fabrication.

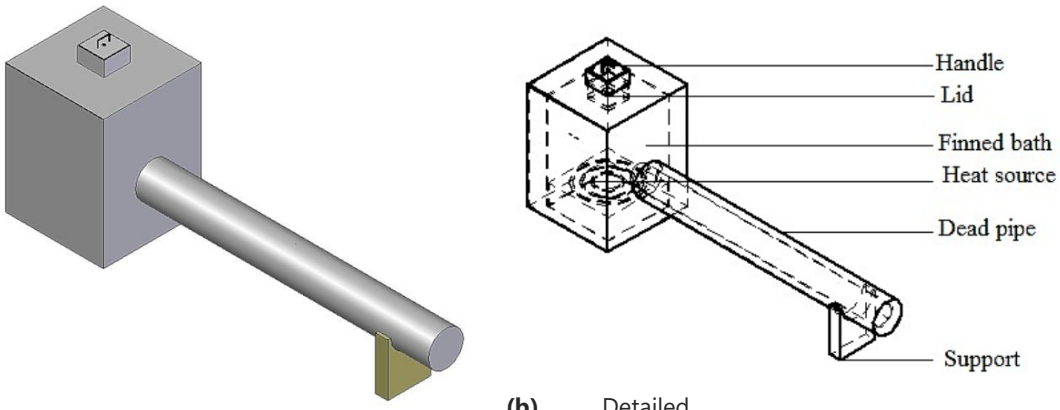

(a) Isometric **(b)** Detailed

Figure 5 Isometric and detailed views of the ITR

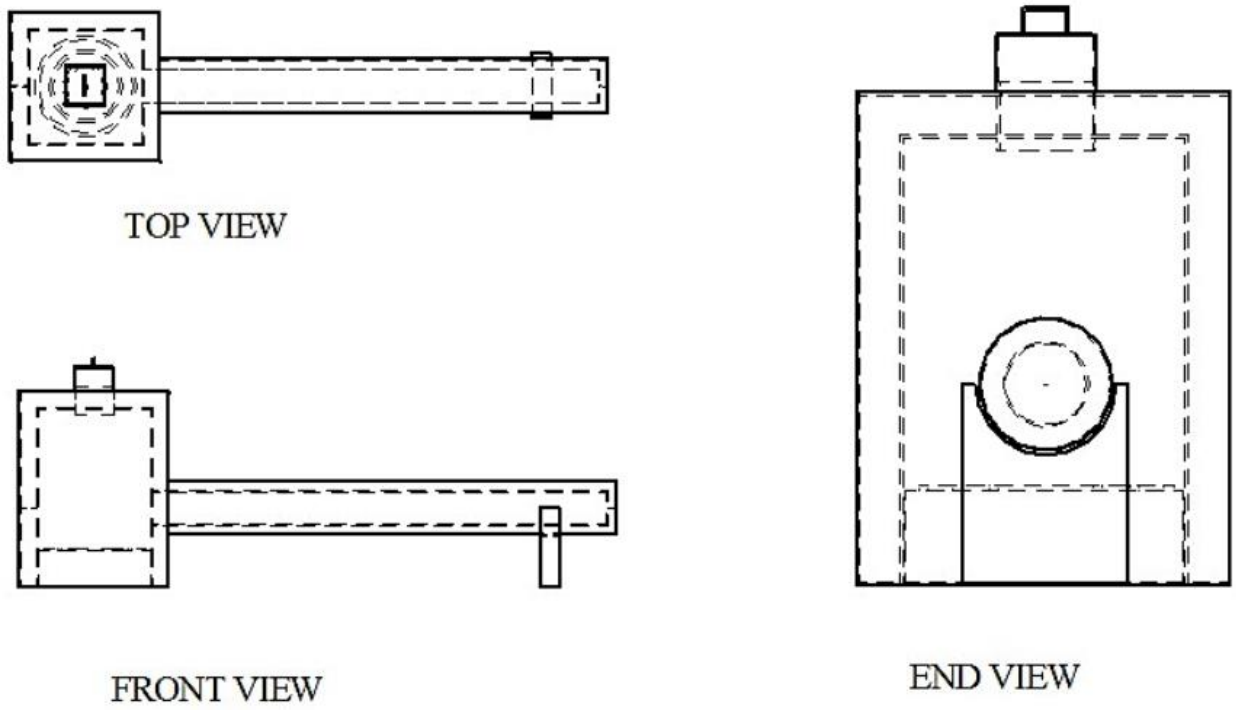

Figure 6 Orthographic view of the ITR

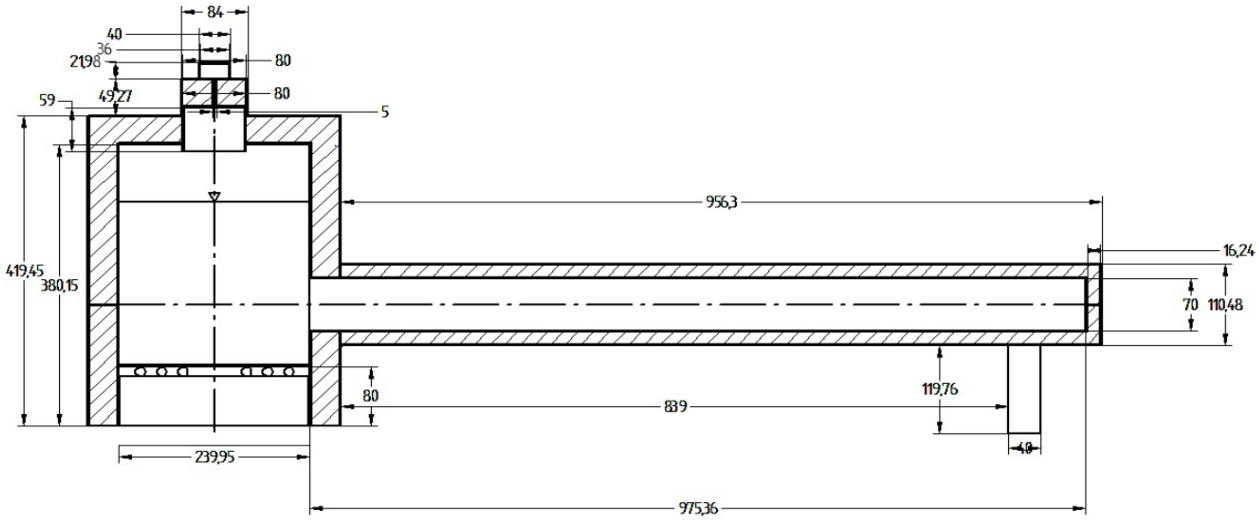

Figure 7 The Front section of the ITR with dimension in millimeter

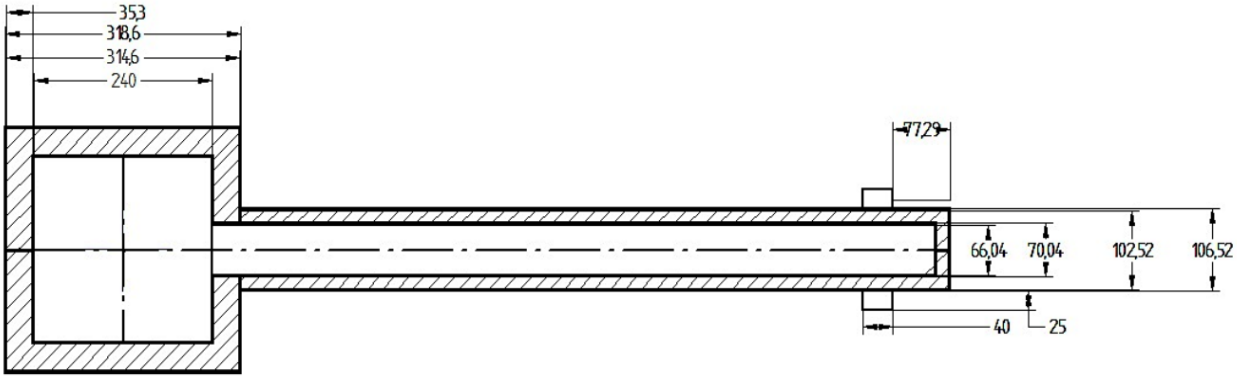

Figure 8 The plan section of the ITR with dimension in millimeter

Figure 9 The pictorial view of the physical ITR

3.4. Equipment costing

Table 6 summaries the unit and total cost of materials which constitute the direct cost. The indirect cost based on standard practice according to Lawal and Ugheoke (2017) is the cost of construction (welding) and spraying the ITR, which is 20% of the total cost of the materials. The grand total is the summation of the individual total costs (direct cost) and construction cost (indirect cost), which yielded 826600 UGX in Table 6.

Table 6 Equipment cost

S#	Material	Dimension	Quantity	Unit cost (UGX)	Total cost (UGX)
1.	Galvanized steel	1219.2×1219.2 m	1	75600	75600
2.	Mild steel	1219.2 × 1219.2 m	1	55000	55000
3.	Heater (hot plate)	0.24×0.24 m	1	40000	40000
4	Rubber clips		6	2000	12000
5.	Insulator (air space)				
6.	Paint (silver colour)				
	Gloss paint	0.001 m^3	1		
	Silver paint	0.001 m^3	1		
7.	Multi-meters:				
	EM420Aallgsun		3	70000	210000
	UNI-T UT33C		4	70000	280000
8.	Welding (Oxy- acetylene)				120000
9.	Coating/spraying				10000
10.	Wooden support		1	4000	4000
11.	Transportation				20000
	Grand total				**826600**

4. CONCLUSION

The design and fabrication of an insulation testing rig has been successfully realized. Three aspects of the designs; the geometric, stress and thermal designs were well articulated in computing the values of the key design parameters; the optimum insulation thickness around the finned bath, the critical insulation thickness around the dead pipe and the thickness of the steel sheet to withstand the maximum allowable stress (Hoop stress) in the ITR.

The optimization of the finned bath component of the ITR was feasible due to the systematic formulation of the design equations for the geometric, stress and thermal designs. Consequently, the optimum insulation thickness at the finned bath was established by simple first order derivative (a gradient method) and the same optimization technique was extended in determining the critical insulation thickness for the dead pipe.

The architectural designs of the ITR was influenced by the optimum insulation thickness around the finned bath, critical thickness of the insulating material around the dead pipe and Hoop supported steel sheet thickness. Furthermore, the design data were translated into several engineering drawings which aided in the fabrication of the physical system of the ITR.

The physical system serves multi-purpose functions; the performance evaluation of insulating materials, estimation of field thermal conductivity of insulating materials and lastly, as laboratory demonstration equipment for heat transfer studies.

Acknowledgement

Authors unanimously acknowledge the management of Kampala International University (KIU) for supporting this research work.

Funding: This research received no external funding.

Conflicts of Interest: The authors declare no conflict of interest.

REFERENCE

1. Abdeen Mustafa Omer. Geothermal Heat Pump Potential and Prospect for Energy Efficient, Sustainable Development, and the Environment. Discovery, 2018, 54(269), 164-188
2. Brown, T. H. 2005."Marks' calculation for machine design." McGraw-Hill Companies, Inc., New York. doi: 10.1036/0071466916
3. Eithun, C.F. 2012. "Development of a thermal conductivity apparatus: analysis and design."Master's Thesis, Norwegian University of Science and Technology E PT-M-2012-27.
4. Engineering ToolBox. 2018. "Stress in Thick-Walled Cylinders - or Tubes."
5. Flori, M.,V. Puţan, and L. Vîlceanu. "Using the heat flow plate method for determining thermal conductivity of building materials." IOP Conference Series: Materials Science and Engineering: 163, 01, 2018.
6. Flynn, D. R., R. R. Zarr, M. H. Hahn, and W. M. Healy. 2002." Design concepts for a new guarded hot sheet apparatus for use over an extended temperature range." Insulating materials: Testing and Applications: 4, 98-115, ASTMSTP 1426, A. O. Desjarlais and R. R. Zarr, eds., ASTM International.
7. Frawley, E., and D. Kennedy. 2007."Thermal testing of building insulating materials." Engineers Journal, 61 (9), 552
8. Gregorec J. 2006: "The Basics of Insulation Testing", IDEAL Industries, Inc., NETA WORLD Fall 2006,
9. https://www.engineeringtoolbox.com/stress-thick-walled-tube-d_949.html (accessed on: 20-09-2018)
10. https://www.netaworld.org/sites/default/files/public/neta-journals/NWFA06_Gregorec.pdf, (accessed on: 13-10-2018)
11. Lawal, S. A., and B. I. Ugheoke. 2017. "Development and performance evaluation of thermal conductivity equipment for laboratory uses." Annals of Faculty Engineering Hunedoara – International Journal of Engineering: 2, 49 – 54
12. Li. M., H. Zhang, and Y. Ju. 2012. "Design and construction of a guarded hot plate apparatus operating down to liquid nitrogen temperature." Review of Scientific Instruments: 83, 075106. https://doi.org/10.1063/1.4732816
13. McMasters, R., Z. J. Harth, and P. T. Taylor, and G. M. Brooke. 2017. "Testing extremely small samples using the flash diffusivity method." International Journal of Numerical Methods for Heat & Fluid Flow: 27 (3), 551-560. https://doi.org/10.1108/HFF-03-2016-0094
14. Nnamchi, S. N., O. D. Sanya, K. Zaina, and V. Gabriel. 2018. "Development of dynamic thermal input models for simulation of photovoltaic generators." International Journal of Ambient Energy." DOI: 10.1080/01430750.2018.1517676
15. Oko, C. O. C., and S. N. Nnamchi. 2012. "Heat transfer in a low latitude flat-sheet solar collector." Thermal science: 16 (2), 583 – 591. DOI: 10.2298/TSCI100419075O
16. Rajput, R.K. 2007. "Engineering thermodynamics." Third Edition, S.I. unit version, LAXMI Publications (P) LTD, New Delhi
17. Salmon, D. 2001. "Thermal conductivity of insulations using guarded hot plates, including recent developments and sources of reference materials." Meas. Sci. Technol.: 12 (12)
18. Simko, T. M., A. H. Elmahdy, and R. E. Collins. 1999. "Determination of the overall heat transmission coefficient (U-Value) of vacuum glazing." A version of this document is published in / Une version de ce document se trouve dans: ASHRAE Transactions: 105 (2), 1-9
19. Sistemas. 2008. "External flow correlations (average, isothermal surface)." http://sistemas.eel.usp.br/docentes/arquivos/5817712/LOQ4086/CorrelationsList.pdf (accessed on: 12-09-2018)
20. Skočilasová, B., J. Skočilas, and J. Soukup. 2018. "Forced convection and heat transfer around a bounded cylinder." MATEC Web of Conferences 157, 02045. https://doi.org/10.1051/matecconf/201815702045
21. Wikipedia 2018. "Overall heat transfer coefficient."https://en.wikipedia.org/wiki/Heat_transfer_coefficient (accessed on 25-10-2018)